



Analysis of planetary boundary layer fluxes and land-atmosphere coupling in the regional climate model CLM

E. B. Jaeger,¹ R. Stöckli,² and S. I. Seneviratne¹

Received 22 December 2008; revised 1 April 2009; accepted 4 June 2009; published 5 September 2009.

[1] Land-atmosphere interactions and associated boundary layer processes are crucial elements of the climate system and play a major role in several feedback processes, in particular for extreme events. In this article, we provide a detailed validation of land surface processes and land-atmosphere interactions in the climate version of the Lokal Modell (CLM), a regional climate model that has been recently developed and is now used by a wide research community. For the evaluation of the model, we use observations from the FLUXNET network and meteorological data. Moreover, we also compare the performance of the CLM with that of its driving data set, the European Centre for Medium-Range Weather Forecasts (ECMWF) operational analysis, and simulations of the Inter-Continental Transferability Study (ICTS). The results show that most of the land-atmosphere coupling characteristics are consistent in CLM and the observations. Nonetheless, the analysis also allows identification of specific weaknesses of the CLM such as an underestimation of the incoming surface shortwave radiation due to cloud cover overestimation, leading to an underestimation of the sensible heat flux. The comparisons with the ECMWF operational analysis and the ICTS models suggest, however, that all models have biases of comparable magnitude. This study demonstrates the utility of flux observations for diagnosing biases in land-atmosphere exchanges and interactions in current climate models and highlights perspectives for our improved understanding of the relevant processes.

Citation: Jaeger, E. B., R. Stöckli, and S. I. Seneviratne (2009), Analysis of planetary boundary layer fluxes and land-atmosphere coupling in the regional climate model CLM, *J. Geophys. Res.*, 114, D17106, doi:10.1029/2008JD011658.

1. Introduction

[2] The future European summer climate is expected to be affected by severe temperature and precipitation changes in the mean as well as in the variability [*Intergovernmental Panel on Climate Change (IPCC)*, 2007, and references therein]. Associated with the simulated changes in variability, climate scenarios project major changes in temperature extremes [e.g., *Schär et al.*, 2004; *Seneviratne et al.*, 2006; *Vidale et al.*, 2007; *Kjellström et al.*, 2007; *Lenderink et al.*, 2007], as well as in precipitation extremes [*Christensen and Christensen*, 2003; *Frei et al.*, 2006], both of which have significant socioeconomic impacts. The underlying mechanisms for changes in extremes are partly linked to changes in large-scale circulation [*Meehl and Tebaldi*, 2004; *Pal et al.*, 2004], as well as effects of clouds on the surface radiative forcing [*Lenderink et al.*, 2007]. However, several investigations have shown recently that land-climate inter-

actions also play a key role for these projections [*Seneviratne et al.*, 2006; *Vidale et al.*, 2007].

[3] Interactions at the interface between the land surface, the planetary boundary layer (PBL), and the overlying atmosphere (hereafter “land-PBL-atmosphere interactions”) are a key aspect not only for changes in future climate but already for the current climate state in transitional climate regions [e.g., *Betts*, 2004; *Koster et al.*, 2004; *Seneviratne et al.*, 2006; *Seneviratne and Stöckli*, 2008]. Of particular importance for land-PBL-atmosphere interactions are clouds, which couple the energy and the water cycles and are still a major source of uncertainty in current climate models according to the latest IPCC report [*IPCC*, 2007]. Over land the cloud cover together with the availability of water for evapotranspiration (E) strongly influences the surface energy budget. Clouds themselves are partly influenced by the availability of water for E, the lifting condensation level, and partly by the large-scale convergence of moisture [*Betts*, 2007]. The availability of water for E over land is primarily linked to precipitation and, hence, again to clouds. The land-PBL-atmosphere coupling involves the numerous complex interactions and feedbacks linked to local soil moisture (SM), cloud, and PBL processes, as well as large-scale dynamics. While possible impacts of SM on temperature are relatively well established [e.g., *Koster et*

¹Institute for Atmospheric and Climate Science, ETH Zurich, Zurich, Switzerland.

²Climate Analysis, Climate Services, MeteoSwiss, Zurich, Switzerland.

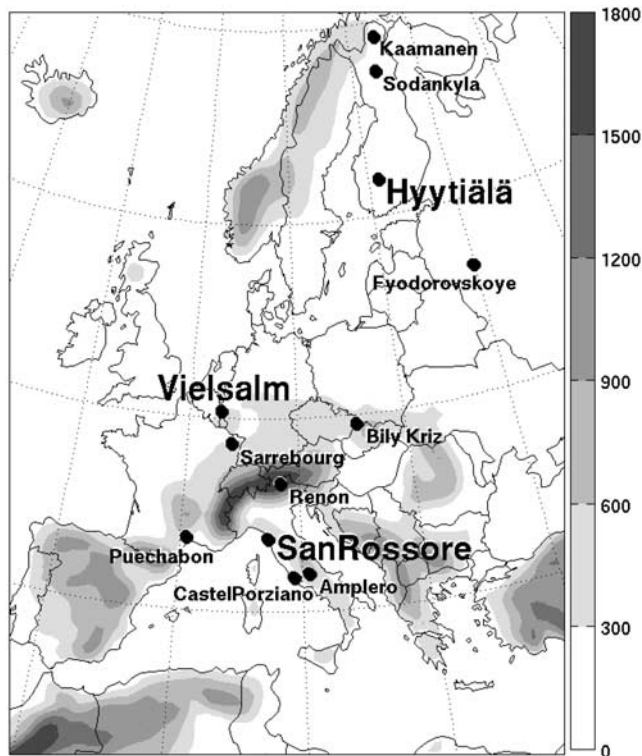


Figure 1. Domain of the CLM simulation with topography (meters). The European FLUXNET sites used in this study are labeled on the map. The three main focus sites are San Rossore (mediterranean climate), Vielsalm (temperate climate), and Hyytiälä (boreal climate).

al., 2006; *Seneviratne et al.*, 2006; *Fischer et al.*, 2007a, 2007b], there are higher uncertainties regarding the impact of SM on precipitation, especially related to convective precipitation and PBL stability [*Findell and Eltahir*, 2003a, 2003b; *Ek and Holtlag*, 2004; *Koster et al.*, 2004, 2006; *Hohenegger et al.*, 2009].

[4] There are several diagnostics to quantify the whole land-PBL-atmosphere coupling or parts of it. For instance, a simple diagnostic was proposed by *Seneviratne et al.* [2006] for diagnosing soil moisture-temperature interactions. They express the sensitivity of E on SM by the correlation of E and 2-m temperature (T_{2M}), $\rho(E, T_{2M})$. Negative $\rho(E, T_{2M})$ are indicative of strong soil moisture-temperature coupling, whereas positive $\rho(E, T_{2M})$ are generally associated with an atmospheric control on E. A recent study by *Koster et al.* [2009] similarly expresses the sensitivity of E to SM using simple indices based on temperature binned by precipitation. In the work of *Ek and Holtlag* [2004] an equation for the relative humidity tendency at the PBL top is proposed, which allows to examine the role of SM and other factors on PBL cloud development. Finally, there is the methodology introduced by Alan K. Betts [*Betts*, 2004; *Betts and Viterbo*, 2005; *Betts et al.*, 2006; *Betts*, 2007], that uses PBL quantities to organize the data (hereafter referred to as Betts analysis).

[5] Owing to the relevance of land-PBL-atmosphere interactions for climate extremes, it is important to validate the associated processes with ground observations. Surface

flux and SM observations, which are crucial for the validation of the relevant processes, are unfortunately very limited both in space and time. FLUXNET observations [e.g., *Baldocchi et al.*, 2001; *Baldocchi*, 2008], which provide observations of water, energy and carbon fluxes based on eddy-covariance measurements over several years, represent a new means to evaluate how land-PBL-atmosphere interactions behave for a particular climate regime, and to validate such processes in a climate model.

[6] In this paper, we illustrate how FLUXNET data can be used for the evaluation and validation of land-atmosphere exchanges and interactions in current climate models. The focus is set on the evaluation of the CLM, a community regional climate model (RCM) used in several research institutions across Europe (<http://www.clm-community.eu/>). The analyzed simulations cover the time period 2002–2005 and are performed over the European continent. Some of the analyses are also extended to the driving model used as boundary condition for the simulations, the IFS forecast analysis (ECMWFop) from the European Centre for Medium-Range Weather Forecasts (ECMWF). Similar analyses could be performed with a larger number of climate models, provided the necessary output data are available.

[7] While grid point validation with observations can provide useful information, it is always unclear whether grid cell model biases can be regarded as representative for larger regions. In our study, we search for systematic model characteristics across climate regimes using data from 12 FLUXNET sites. We focus in particular on the Hyytiälä, Vielsalm and San Rossore sites as representative for the northern European boreal climate, central European temperate climate, and southern European mediterranean climate, respectively (Figure 1). Since land-surface processes play an important role primarily in summer, the analysis is mainly focused on the warm season.

[8] The paper is organized as follows: Section 2 presents the data sets and the general methodology applied in this study. Then, in section 3, the surface fluxes of CLM and ECMWFop are validated. Section 4 addresses the links between surface, PBL and cloud processes by stratifying the data by soil moisture and cloud cover on both monthly and daily time scales. Finally, the main results are summarized in section 5.

2. Data and Methodology

2.1. Data: Models

2.1.1. CLM

[9] We investigate here the CLM RCM, which is the climate version of the COSMO model (Consortium for Small-scale Modeling) employed by several European weather services for numerical weather prediction. Our model configuration is similar to that used for the EU-FP6 project ENSEMBLES [*Jaeger et al.*, 2008]: CLM 2.4.11 with 0.44° (≈ 50 km) horizontal resolution, 32 levels in the vertical, 10 soil layers, and a model time step of 240 s. (*Jaeger et al.* [2008] use CLM version 2.4.6, which is basically the same as the version used in this study. Additionally, we have corrected for the missing restriction of evapotranspiration below the plant wilting point.) The domain covers the entire European continent, from Iceland

Table 1. Overview of the Flux Towers Used in This Study^a

Site and Reference	Short	Lon (°E)	Lat (°N)	Alt (m)	Biome Type	Years	Climate Zone (Köppen)
BilyKrizForest [Reichstein et al., 2005]	CZBK1	18.54	49.50	908.0	Evergreen	2002–2005	Hemiboreal (Dfb)
CastelPorziano [Reichstein et al., 2002]	ITCpz	12.38	41.71	68.0	Evergreen	2002–2005	Mediterranean (Csa)
Sarrebourg [Granier et al., 2000]	FRHes	7.06	48.67	300.0	Deciduous	2002–2005	Maritime temperate (Cfb)
Hyytiälä [Suni et al., 2003]	FIHyy	24.29	61.85	181.0	Evergreen	2002–2005	Boreal (Dfc)
Kaamanen [Laurila et al., 2001]	FIKaa	27.30	69.14	155.0	Wetland/Tundra	2002–2005	Boreal (Dfc)
Puechabon [Reichstein et al., 2002]	FRPue	3.60	43.74	270.0	Deciduous	2002–2005	Mediterranean (Csa)
Renon [Marcolla et al., 2005]	ITRen	11.43	46.59	1730.0	Evergreen	2002–2005	Hemiboreal (Dfb)
SanRossore [Reichstein et al., 2005]	ITSRo	10.29	43.73	4.0	Evergreen	2002–2005	Mediterranean (Csa)
Sodankyla [Hatakka et al., 2003]	FISod	26.64	67.36	180.0	Evergreen	2002–2005	Boreal (Dfc)
Vielsalm [Aubinet et al., 2001]	BEVie	6.00	50.31	450.0	Mixed	2002–2005	Maritime temperate (Cfb)
Amplero [Gilmanov et al., 2007]	ITAmpl	13.61	41.90	884.0	Grassland	2002–2005	Humid subtropical (Cfa)
Fedorovskoye [Milyukova et al., 2002]	RUFyo	32.92	56.46	265.0	Evergreen	2002–2005	Hemiboreal (Dfb)

^aMain focus sites are denoted in bold. Abbreviations: Lon, longitude; Lat, latitude; Alt, altitude.

to the Black Sea, and from northern Africa to northern Russia (see Figure 1 for a map). The setup uses external parameters derived from AVHRR data for the vegetation parameters (leaf area index, plant cover and root depth) and from the FAO 1995 digital soil map for soil types (9 classes in CLM). Lateral boundary conditions are derived from ECMWFop, whereas the initial conditions correspond to the climatological values of a long-term CLM simulation driven with ERA40 reanalysis [Uppala et al., 2005] to ensure that the model is approximately within its equilibrium.

[10] Our CLM configuration uses Leapfrog numerics, a radiative transfer scheme based on work by Ritter and Geleyn [1992], Tiedtke [1989] convection based on a moisture-convergence closure, vertical turbulent diffusion using prognostic TKE [Raschendorfer, 2001], and a second-generation multilayer soil model TERRA-ML (BATS) [Schrodin and Heise, 2002] with both bare-soil evaporation and transpiration being calculated following Dickinson [1984]. More details on the model dynamics and physics are available from Steppeler et al. [2003] and A. Will et al. (Physics and Dynamics of the CLM, submitted to *Meteorologische Zeitschrift*, 2009). In addition, model documentation, source code and community information can be found on the CLM (<http://www.clm-community.eu/>) and COSMO (<http://cosmo-model.cscs.ch/>) web pages.

2.1.2. ECMWFop

[11] The ECMWFop data set is used for the lateral boundary conditions of the CLM simulation. Moreover, it is also validated here against observations and compared to CLM, using monthly mean fields from the ECMWF MARS archive (<http://www.ecmwf.int/services/archive/>). The underlying model of the ECMWFop for the period 2002–2005 is the IFS model using a 4D-Var data assimilation technique, a horizontal resolution of T_L511 and 60 levels in the vertical on a hybrid sigma-pressure coordinate (in its latest version, IFS CY31r1, the resolution is T_L799 with 90 levels). However, in contrast to the ERA40 reanalysis, the model used to calculate ECMWFop is continuously being adapted to the latest model developments (changed twice within the period of interest, i.e., 2002–2005).

2.1.3. ICTS Model Simulations

[12] To compare the performance of CLM to other state-of-the-art RCMs, data from the GEWEX-CEOP ICTS project (Inter-Continental Transferability Study) is analyzed here for the period 2002–2003 [e.g., Rockel et al., 2006; Takle et al., 2007]. The following NCEP2 reanalyses driven models were used: CLM (simulation from GKSS Research

Centre, Germany), CRCM (OURANOS, Canada), GEM-LAM (RPN/MSC and University of Quebec, Canada), and the RSM (Experimental Climate Prediction Center, U.S.). The ICTS CLM simulation slightly differs from the one that we have performed: version 2.4.6, NCEP2 reanalysis boundary data, spectral nudging and ECOCLIMAP vegetation parameters. Detailed information on the models and their setup can be obtained from <http://icts.gkss.de>.

2.2. Data: Observations

2.2.1. FLUXNET

[13] For the model validation and the process analysis, we use measurements from the FLUXNET Level 2 flux tower data sets listed in Table 1 (for more details, e.g., concerning the instruments, we refer the reader to the respective publications and references therein, or to the official FLUXNET homepage <http://www.fluxnet.ornl.gov>). In total, data from 12 stations are assessed covering a range of different climatic regimes, though the main focus is on the Hyytiälä, Vielsalm and San Rossore sites (with the exception of Figure 6). The selection of the stations is based on maximum spatial and temporal data coverage across Europe. None of the validation data were gap-filled and comparison to the model output is only done at times when no gaps occur. In contrast to the study of Stöckli et al. [2008], no u^* screening for measurement error reduction was performed owing to the fact that some of the data used in this study are not available on submonthly or subdaily resolution. (In order to account for biases in LE and H measurements during periods of low turbulence, it is a common approach to compare model to measurements only for times when the u^* value (friction velocity) is large [Schmid et al., 2003; Stöckli et al., 2008]. This procedure reduces the systematic error in measured surface fluxes due to failure in energy balance closure.) Moreover, appropriate choice of u^* values is not straightforward. However, a comparison of FLUXNET and CLM fluxes with and without u^* screening reveals no systematic differences in the results, beside generally larger fluxes for u^* -screened data. We assess amplitude errors only in the first part of the study (Figures 2, 3, and 4). Therefore, the systematic error due to the well-known failure in energy balance closure of the eddy-covariance measurement technique (for a concise review on this problematic, see Foken [2008]) has been estimated by adding the residual of the energy balance closure for each site to the surface fluxes according to the Bowen ratio (B; see shaded area in Figures 2, 3, and 4). (Though some studies report larger systematic measurement

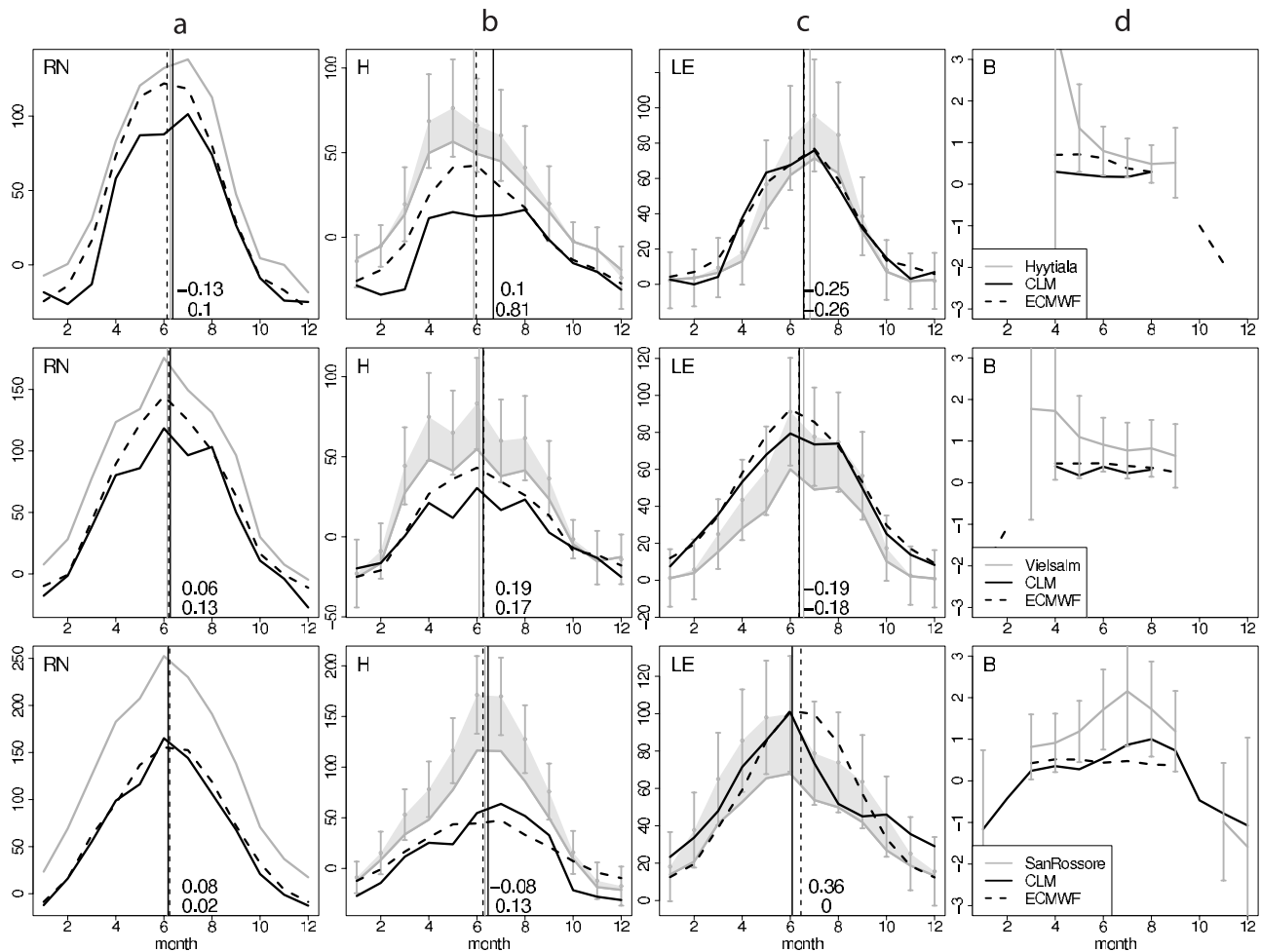


Figure 2. Mean seasonal cycle of (a) RN, (b) H, (c) LE (all in W m^{-2}), and (d) B (no unit) at (top) Hyytiälä, (middle) Vielsalm, and (bottom) San Rossore for the years 2002–2005. Shown are FLUXNET observations (grey line), ECMWF (black dashed line), and CLM (black solid line) model data. The error bars are a rough estimate of the random measurement error, and the grey shadings indicate a rough estimate of the systematic error due to nonclosure of the energy balance. Additionally, the phase-shift error is shown by vertical lines (top number is for ECMWF, and bottom number is for CLM).

errors for LE than for H [e.g., *Finkelstein and Sims, 2001*], correction of closure according to B is a reasonable approach in the absence of complementary information [*Twine et al., 2000*].) The residual was calculated from a robust linear regression of hourly observed net radiation (RN) versus LE, H and ground heat fluxes [*Wilson et al., 2002*; *Stöckli et al., 2008*]. Beside this systematic error, random measurement errors in turbulent surface fluxes were estimated on the basis of empirical findings by *Richardson et al. [2006]* and are displayed as error bars in Figures 2, 3, and 4.

2.2.2. Basin-Scale Estimation of Evapotranspiration

[14] Evapotranspiration is alternatively calculated using the atmospheric water-balance equation for individual catchments [e.g., *Yeh et al., 1998*; *Hirschi et al., 2007*; *Jaeger et al., 2008*] using precipitation from E-OBS gridded data set (see below) and further estimates from the ECMWF model (Figure 5). Regarding atmospheric water balance estimates based on ECMWF data, see, for example, *Senviratne et al. [2004]* and *Hirschi et al. [2006a, 2006b]*, and regarding a discussion of the associated uncertainties we

refer the reader to *Jaeger et al. [2008]* and references therein.

2.2.3. E-OBS

[15] For the derivation of the atmospheric water balance estimates of E, as well as for the analysis of the 2003 European summer heat wave (see Figure 10), the gridded E-OBS precipitation and T_{2M} data from the EU-FP6 project ENSEMBLES were used [*Haylock et al., 2008*].

2.3. Analysis Methodology

[16] In the analysis, we mainly focus on the evaluation of the model data with the FLUXNET measurements. The comparisons were done by taking the closest model land grid point to the FLUXNET sites. We did additional tests using a weighted average of the surrounding grid cells, but did not find marked differences in the results (not shown). For the comparison with the atmospheric water balance estimates, the model data were aggregated on the corresponding river basins.

[17] First, in section 3, we validate the mean seasonal and diurnal cycles of RN, LE and H of CLM using data from

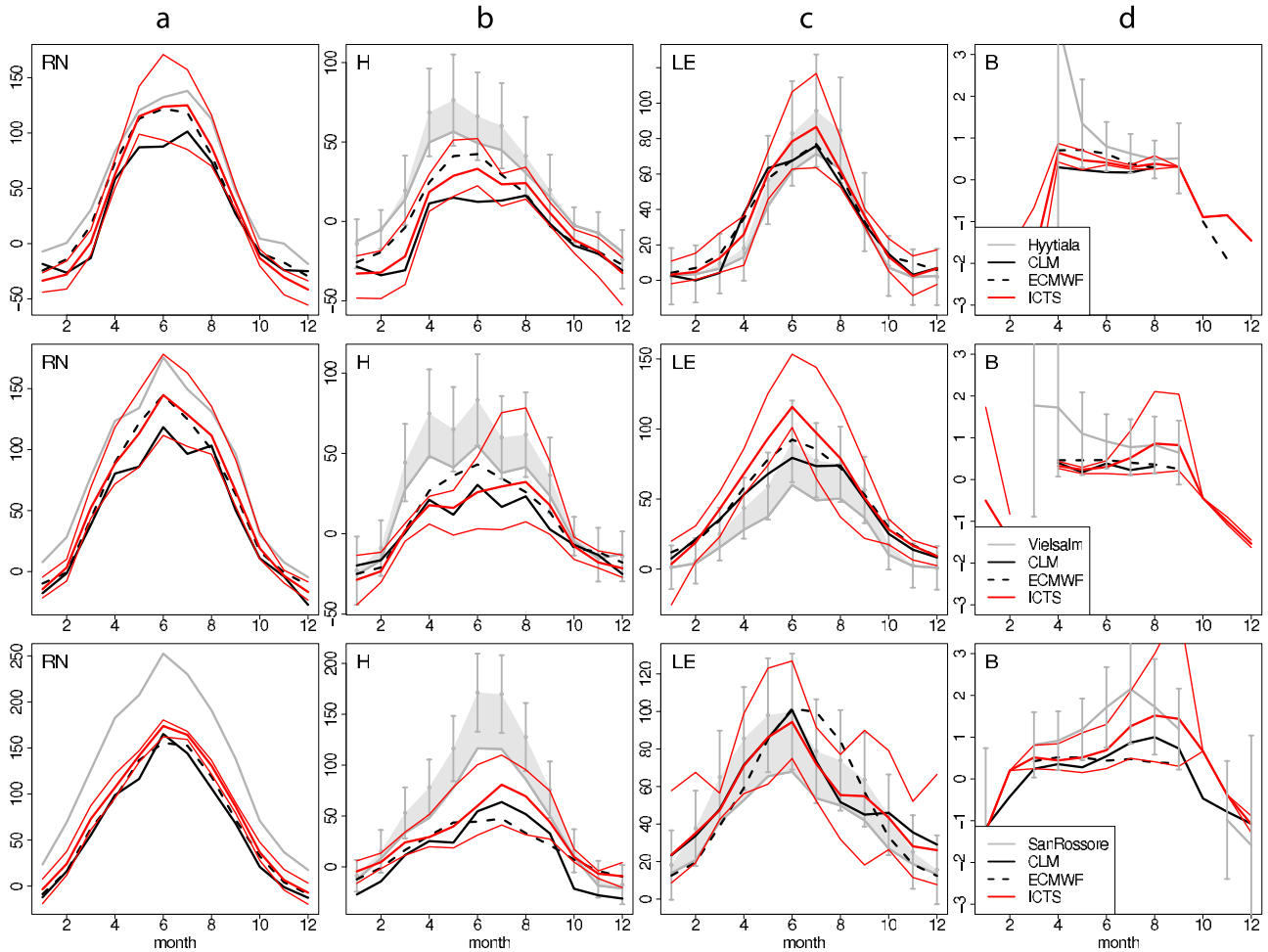


Figure 3. Same as Figure 2 but including the mean of the ICTS models and the respective maximum and minimum monthly value for the years 2002–2003.

FLUXNET. We analyze amplitude as well as phase-shift errors. The seasonal cycle is additionally compared to the ECMWFop and the ICTS models, and in the case of E compared to the atmospheric water balance estimates. Then, in a second part (section 4), we assess if CLM and ECMWFop reasonably represent the land-PBL-atmosphere coupling compared to FLUXNET data. For this, we use the coupling diagnostic proposed by *Seneviratne et al.* [2006] for soil moisture-temperature coupling, and follow the Betts analysis regarding temporal relationships between variables at the land-PBL-atmosphere interface (see section 1). In the latter analyses, we use soil moisture (SM) and cloud albedo (α_{cloud}) to organize the data. Using the organized data, the coupling of SM and α_{cloud} to the meteorological quantities RN, LE and H is diagnosed. We refer here to correlation relationships as “coupling,” though one should note that, owing to the complexity of the climate system, causality is never clear. Here are the main rationales for focusing on SM and α_{cloud} :

[18] 1. Soil moisture (SM) is often the main quantity limiting E and, hence, controlling the partitioning of incoming energy into LE and H. We use the following SM index in order to get a meaningful quantity to compare

model data against observations for a range of different climate zones,

$$SMI = \frac{SM - SM_{\min}}{SM_{\max} - SM_{\min}}, \quad (1)$$

where SM_{\max} and SM_{\min} denote the maximum or minimum SM value of the model or the observations (wherever the analysis is based on daily values, SMI is calculated from daily SM values, otherwise from monthly means).

[19] 2. Cloud albedo (α_{cloud}) will be used as a quantitative measure of the cloud field. Clouds are fundamental quantities of the climate system, owing to their strong impact on surface radiation. The latter again feeds back on clouds via surface heat and moisture fluxes. We ignore multiple reflections and calculate α_{cloud} after *Betts et al.* [2006],

$$\alpha_{cloud} = 1 - \frac{SW_{dn}^{all}}{SW_{dn}^{clear}}, \quad (2)$$

with $0 < \alpha_{cloud} < 1$. This transformation removes the large seasonal variation of clear-sky fluxes associated with changing solar zenith angle. Note that this definition does not only

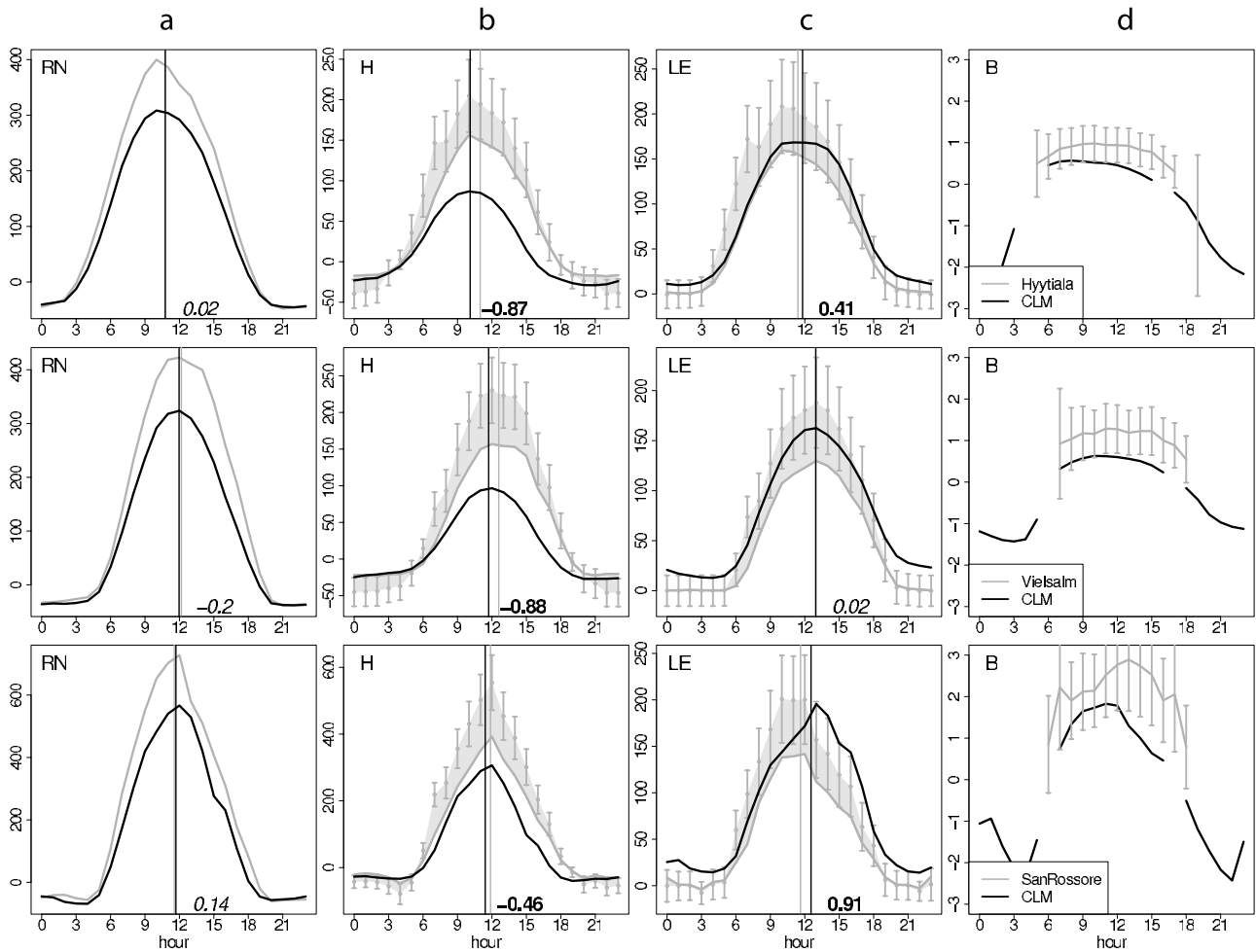


Figure 4. Same as Figure 2 but for mean diurnal cycles of July and without ECMWF data. Additionally, the phase-shift errors in bold numbers are statistically significant on the 5% level according to a bootstrap resampling test (500 samples).

include radiation reflection (albedo) but also absorption within the cloud. (Clear-sky fluxes (S) were estimated both for model and observations using $S = S_0 \cos(z) T^m$, where S_0 denotes the solar constant (1368.0 W/m^2), z the zenith angle, T the atmospheric transmittance (0.82) and m the relative optical air mass according to a formulation based on work by

Young [1994]. The zenith angle is calculated depending on position (latitude, longitude and height) and time after Reda and Andreas [2003].)

[20] The relative humidity (RH) is another key PBL quantity and linked to several PBL processes. As shown in the investigations of Betts *et al.* [2006] and Betts [2007],

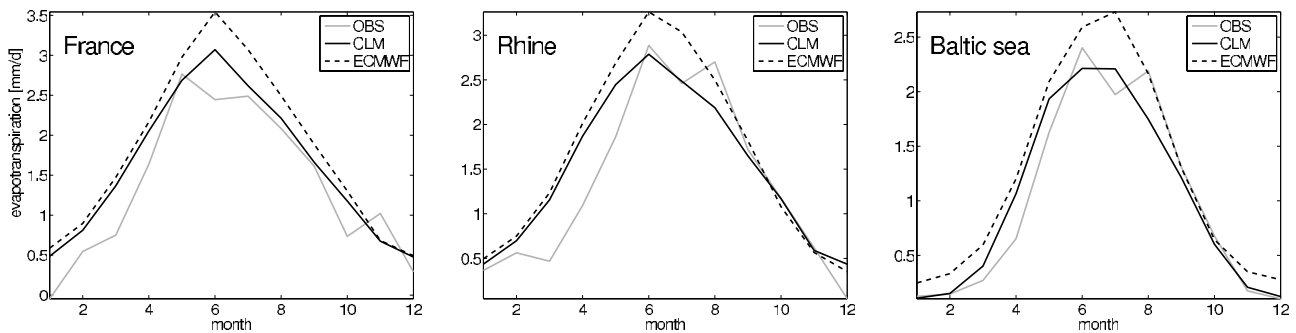


Figure 5. Validation of evapotranspiration (mm d^{-1}) for European river catchments using estimates based on the atmospheric water balance: (left) France, (middle) Rhine, and (right) Baltic Sea catchments for the years 2002–2005.

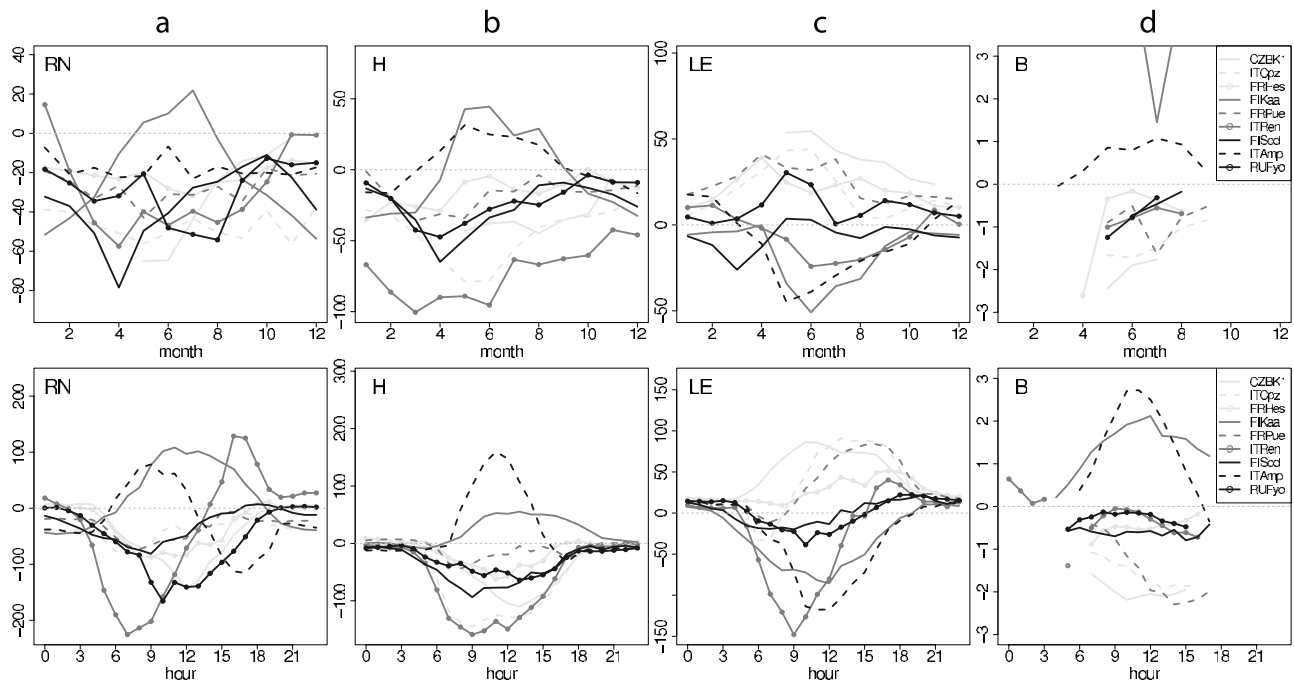


Figure 6. Same as in (top) Figure 2 and (bottom) Figure 4 but for the CLM bias at the other stations (see Figure 1) and without error estimates.

near-surface RH is closely related to the height of the lifting condensation level, which is an estimate of the mean height of the cloud base, and therefore to the processes that control the equilibrium of the PBL on daily timescales. However, since RH, SM and α_{cloud} have a quasi-linear relationship, stratification by RH gives similar results as for SM or α_{cloud} , and will therefore not be shown hereafter.

3. Validation of Surface Fluxes

[21] This section presents the validation of the surface fluxes in CLM. First, in Figure 2, we display the mean seasonal cycle of RN, H, LE and B in CLM and ECMWFop for the time period 2002–2005. The CLM seasonal cycle is compared to that of the ICTS models for the period 2002–2003 in Figure 3, and it is also independently evaluated with atmospheric water-balance estimates (see section 2.2.2) in Figure 5. In addition, we provide an analysis of the diurnal cycles of RN, H, LE and B in CLM in Figure 4. The main focus is on the boreal climate site Hyytiälä, the temperate climate site Vielsalm and the mediterranean climate site San Rossore, but a summary of CLM biases at all sites is provided in Figure 6.

3.1. CLM Seasonal Cycles

[22] A first marked feature of Figure 2 is the systematic underestimation of RN in CLM, which can be attributed to an overestimation of total cloud cover as already discussed by Jaeger *et al.* [2008]. Interestingly, the missing incoming energy is not equally distributed onto LE and H. If random and systematic measurement errors are taken into account, it can be stated that H is underestimated in CLM (primarily in summer), whereas LE is generally within the uncertainty range and, hence, that B is slightly underestimated. Two sites show a different behavior (Figure 6): At Amplerio, CLM overestimates H and strongly underestimates LE

(likely owing to the drying out of soils in summer), and at Kaamanen, CLM overestimates RN and also underestimates LE (note that both stations have a large fraction of missing data values in the observations). The systematic bias in B is in line with findings of a recent study by Brockhaus *et al.* [2008] using a similar CLM setup: Several central European profiles show a cold and often also moist bias throughout the PBL in summer if the Tiedke convection scheme with moisture convergence closure is used. Other convection schemes or closures give more realistic PBLs, though often for the wrong reason and at the expense of the precipitation performance.

[23] Despite the uncertainty in the absolute magnitude of eddy-covariance measurements, the timing and phase of the seasonal cycles can be analyzed. The general course looks reasonably good for the CLM fluxes. The phase-shift error is quantified by defining the peak of the seasonal cycle as the time at which half of the total RN, H or LE flux has been measured or modeled (calculated by the area below the curve). For the mean seasonal cycles no systematic phase-shift errors can be identified (indicated in Figure 2 by decimal months). However, there is a tendency for H to have a positive and LE to have a negative phase-shift error compared to FLUXNET observations. This appears to be due to a too early onset of the vegetation period in spring, though the phase shifts are usually small for LE (<0.4 months) but for some stations quite large for H (≈ 1 month).

3.2. Comparison With ECMWFop and ICTS Models

[24] Figure 2 also shows the corresponding curves of RN, H, LE and B for ECMWFop. Again the closest land grid point was chosen for the analysis. Generally, ECMWFop produces a more accurate seasonal cycle of RN than CLM, although RN is still systematically underestimated. This could be partly attributed to a SW_{dn} underestimation of

the ECMWF model. A comparison to data from the Global Energy Balance Archive (GEBA) observational data set [Gilgen and Ohmura, 1999] indicates indeed such an underestimation for most parts of Europe (not shown). Because of the smaller bias in RN, H is closer to the observed values for most stations in ECMWFop, but similarly to CLM usually below the FLUXNET observations. LE in ECMWFop is close to that of CLM and within the measurement uncertainty. In general, H and particularly LE are both smaller in CLM than in ECMWFop owing to the strong RN underestimation in CLM. The ECMWFop B is similar to that of CLM (underestimation), but somewhat closer to the observations (in general slightly larger except for southern Europe in summer). Akin to what was identified for CLM, there is a tendency in ECMWFop for H to have a positive and LE to have a negative phase-shift error compared to the FLUXNET measurements.

[25] In order to evaluate to which extent the CLM biases are of comparable magnitude to that of other available RCMs, we provide a comparison with the ICTS model simulations in Figure 3. Figure 3 displays the seasonal cycle of CLM, and of the ICTS models mean, min and max values for the years 2002–2003. The RN underestimation is not systematic for the ICTS models (except in winter), and appears thus to be a specific feature of the CLM model. This can be partly understood by the total model cloud cover, that is much larger in CLM than in the other RCMs (not shown) and has a large effect on RN. By contrast, some of the ICTS models (ECPC and RPNMSC) overestimate RN, particularly in summer. Therefore, the ICTS model mean has slightly larger values of LE and H than CLM. However, all models appear to underestimate B (at least in spring and at the beginning of summer). Since the underestimation of B is rather small and the measurement errors in LE and H are large and associated with uncertainties, it is possible that this underestimation is not significant. It appears that all models have a too early onset of the vegetation period resulting in a too early onset of LE and delayed onset of H in spring.

[26] As an alternative source of E observations, we use atmospheric water-balance estimates (section 2.2.2) for the following European river basins or regions: the Baltic Sea (northern Europe), the Rhine river basin (central Europe), and France (aggregation of river basins). As shown in Figure 5, the seasonal cycle of CLM is in good agreement with this data set. In contrast, ECMWFop generally overestimates E in summer. The ERA40 reanalysis (based on an earlier version of ECMWFop) suffers from a similar overestimation of E in the Baltic Sea catchment ($\approx 20\%$) and in the Danube catchment ($\approx 8\text{--}35\%$) as found by Hagemann *et al.* [2005]. The ECMWFop modeled E (and consequently LE) also has a negative phase-shift error compared to the E estimation of the analyzed catchments (not shown).

[27] In summary, the evaluation of the CLM fluxes suggests that RN is unambiguously underestimated, and results in an underestimation of H. LE on the other hand is generally within the measurement uncertainty of the FLUXNET data, as well as reasonably modeled in comparison to the atmospheric water-balance estimates. There is, however, strong evidence for a negative phase shift in LE. The underestimation of H and correct representation of LE result in an underestimation of B. Note that the RN, H and B underestimation can be partly corrected with an increase of

the minimal stomatal resistance in CLM (not shown). The minimum stomatal resistance is specified as a constant for all soil (/land cover) types in CLM. The German weather service (COSMO model developer) is currently working on a map for a soil (/land cover) type-dependent minimal stomatal resistance, with indeed generally larger values than those used in the CLM version analyzed here (J. Helmert, personal communication, 2008).

3.3. CLM Diurnal Cycles

[28] In Figure 4 the mean diurnal cycles in July for the period 2002–2005 are shown for CLM and the FLUXNET observations at Hyytiälä, Vielsalm, and San Rossore. Similarly to the biases of the mean seasonal cycle, RN is systematically underestimated during daytime for all months and sites, whereas nighttime biases are varying across sites and months, but are mostly negative as well. Again, the missing energy is not equally distributed among LE and H, and mostly affects H. While the LE fluxes are generally within the uncertainty range of the observations, H is again systematically underestimated during daytime for all months and sites. As for the seasonal cycle, Kaamanen and Amplerio exhibit a different behavior (overestimation of H, Figure 6). The phase-shift errors in the diurnal cycle are generally larger than for the seasonal cycles, with phase-shift errors of LE being systematically and (often also significantly positive (indicated in Figure 4 by decimal hours: $\approx 0\text{--}2$ h)). The same holds for RN for most stations and months, whereas phase-shift errors of H are mostly negative. Note that the larger sample size of July diurnal cycles (4 years times 31 days) compared to the one of the seasonal cycles (only 4 years) allows for reasonable testing of statistical significance. Therefore, we use a block bootstrap resampling test by sampling 500 times with replacement from all July diurnal cycles (4×31).

4. Coupling of Cloud and Surface Processes

[29] In this section we investigate the quality of the modeled coupling of PBL processes in CLM, and partly also in ECMWFop, and compare the model results to FLUXNET observations. It is not possible to show the whole suite of diagnostics proposed by the Betts analysis, because some necessary variables are not available from the observations. However, an additional dimension is added in our analysis compared to the mentioned studies, because we investigate the coupling diagnostics under three different climate regimes (mediterranean, temperate, boreal). This allows us to account for a further aspect of climate variability than single-site studies. As stated already by Betts [2007], the land-PBL-atmosphere system is a highly coupled one, and while the shown results are suggestive of important interactions within the system, they do not show a clear “direction of causality.” In addition to the Betts coupling diagnostics, we also investigate soil moisture-temperature coupling in CLM in section 4.1 following a similar approach to that proposed by Seneviratne *et al.* [2006].

4.1. Correlation of Temperature and Latent Heat Flux

[30] In Figure 7 we compare the monthly correlation between LE and T_{2M} , $\rho(\text{LE}, T_{2M})$, in CLM, ECMWFop

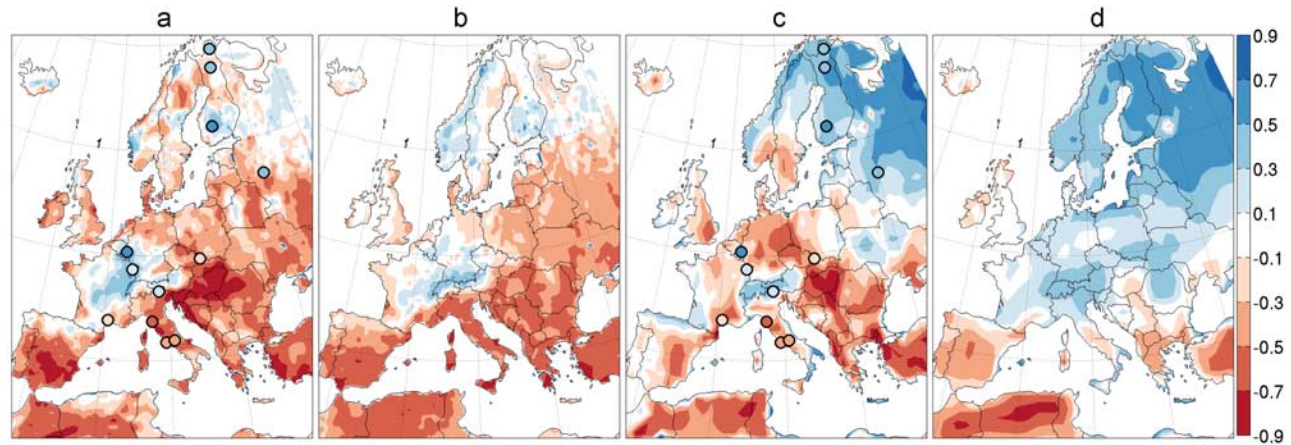


Figure 7. Correlation of summer T_{2M} and LE for the period 2002–2005 for (a) CLM and (c) ECMWFop and for the period 1959–2006 for (b) CLM and (d) ECMWFop. The circles indicate the corresponding correlations from the FLUXNET observations.

and in the FLUXNET observations during the summer months (June, July, August). As proposed by *Seneviratne et al.* [2006], $\rho(\text{LE}, T_{2M})$ can be seen as a reverse measure of soil moisture-temperature coupling, as negative correlations point to a strong control of SM upon LE and T_{2M} , while positive correlations generally point to a strong atmospheric control on LE. Note that we apply this coupling diagnostic on a different time scale than in that study, since we consider here monthly rather than seasonal E and T_{2M} (owing to the short length of the simulations). However, if the two computation approaches are compared for long-term simulations, no notable differences are found (not shown). For CLM, there is a good agreement with the observed values of $\rho(\text{LE}, T_{2M})$, except for the boreal stations Kaamanen, Sodankyla and Fedorovskoje. Consistent with *Seneviratne et al.* [2006], strongest coupling (negative $\rho(\text{LE}, T_{2M})$) is found in the Mediterranean region (e.g., San Rossore), which is a transitional zone between dry and wet climates. On the other hand, regions with stronger atmospheric control on LE (positive $\rho(\text{LE}, T_{2M})$) are located in central Europe (e.g., Vielsalm) and at several spots in Scandinavia (e.g., Hyytiälä). Though the correlation is based on only 12 summer months (2002–2005), it is still robust as indicated by the corresponding plot for a longer-term correlation (1959–2006, Figure 7b). For ECMWFop, there is a better agreement with the observations in northern Europe, whereas there are erroneous correlations compared to central European stations (e.g., Vielsalm). This might be caused by the nonrobustness of the small sample correlation (2002–2005) compared to the longer-term correlation (1959–2006) for that data set (though this was not the case for CLM). Overall, this comparison suggests that CLM has reasonable features regarding monthly soil moisture-temperature coupling in summer. For a comparison of $\rho(\text{LE}, T_{2M})$ derived from the PRUDENCE RCMs (<http://prudence.dmi.dk/>) with those of CLM see *Fischer and Schär* [2009, Figure 4].

4.2. Seasonal Cycles as a Function of Soil Moisture

[31] Before we start to use daily data to quantify the land-PBL-cloud field coupling, we display the mean seasonal

cycles as a function of SMI (see equation (1)). The curves are more “noisy” than those presented by *Betts and Viterbo* [2005] owing to the small sample size (4 years compared to 12 years in their study). Moreover it should be kept in mind that SM is a spatially highly varying quantity and, hence, the question of representativeness is particularly an issue for SM owing to the large spatial gap between local observations and the climate models.

[32] In Figure 8, mean seasonal cycles of RN, H, LE and α_{cloud} are plotted as a function of SMI for the period 2002–2005. Again Hyytiälä, Vielsalm and San Rossore are shown as examples for boreal, temperate and mediterranean climate, respectively. The starting of the arrow denotes January, the endpoint December, the first cross June and the second July. The numbers in the lower left corner of each plot in Figure 8 give the respective correlation coefficient (R) for CLM (black), ECMWFop (dark grey) and the observations (light grey). The correlation was tested for significance on the 5% level using a randomization test. The biases of CLM in RN, LE and H are again visible, but will not be discussed in more detail hereafter, since we focus here on the coupling between the processes rather than the mean fluxes. Generally speaking, RN, LE and H are smallest in winter and largest in summer. SM on the other hand is largest in winter and smallest in summer only in southern Europe, whereas toward the north this clear seasonal cycle is reduced. For its part, α_{cloud} is largest in winter and smallest in summer in southern Europe, but is on the contrary smallest in winter and largest in summer in northern Europe. The curves are far away from a single path, which is mainly owing to the fact that the relationship of SM with the other variables varies over time, and in particular as a function of the seasonal cycle (owing to variations in vegetation activity).

[33] An interesting feature is the stronger coupling of RN, LE and H to SM toward southern Europe as indicated by the stronger correlations, which also holds for the other sites. This corresponds well with the stronger coupling between SM and temperature diagnosed in the Mediterranean from $\rho(\text{LE}, T_{2M})$ in Figure 7, and with the expected stronger

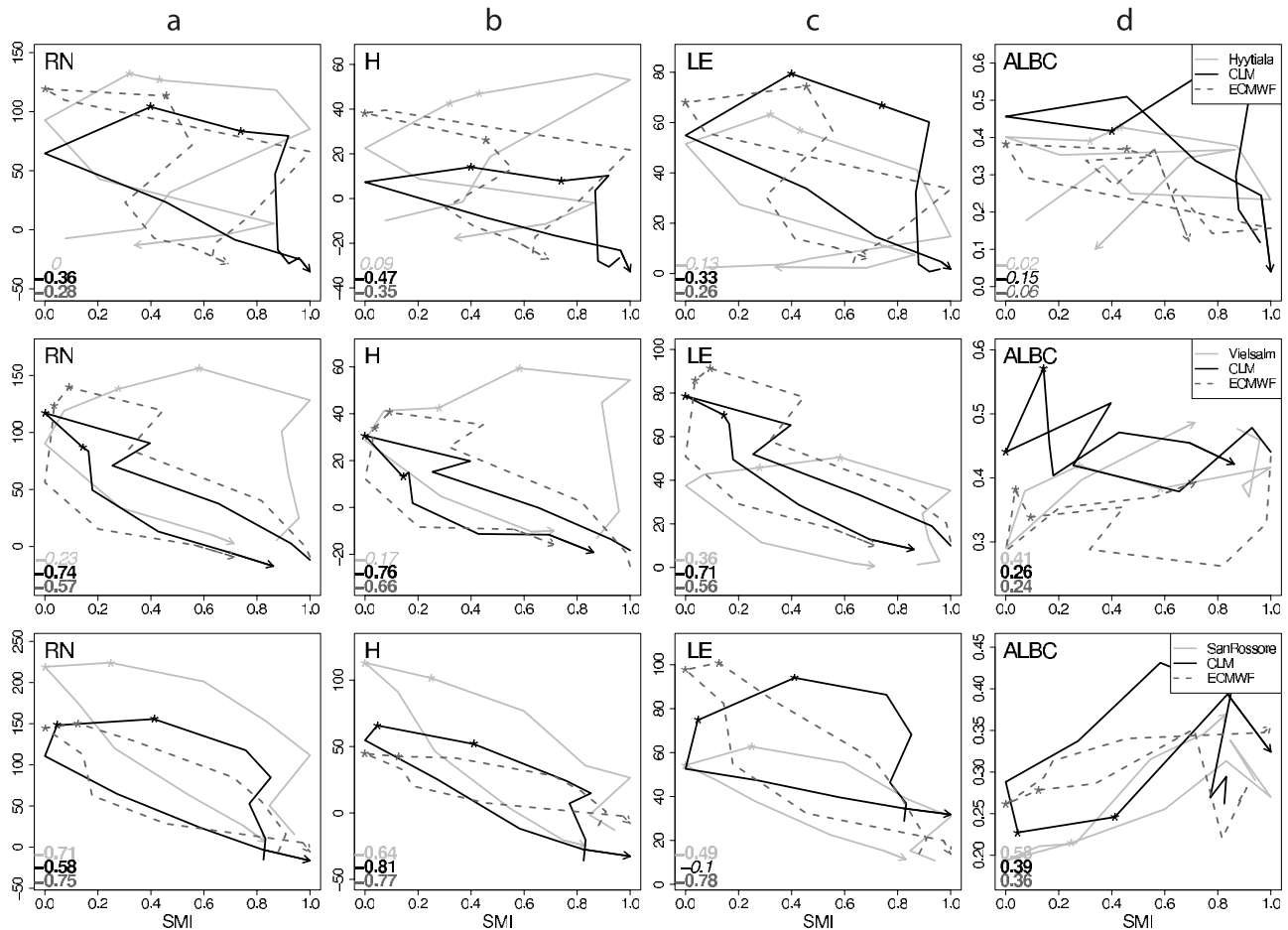


Figure 8. Mean seasonal cycle for the years 2002–2005 of (a) RN, (b) H, (c) LE (all in W m^{-2}), and (d) α_{cloud} (no unit) as a function of SMI (no unit). The correlation coefficient (R) is given in the lower left corner of each plot (first number is FLUXNET, second is CLM, and third is ECMWF), with bold numbers being statistically significant on the 5% level according to a randomization test (10,000 samples). Shown are (top) Hyytiälä (boreal climate), (middle) Vielsalm (temperate climate), and (bottom) San Rossore (mediterranean climate).

SM-climate coupling in transitional climate regions [e.g., Koster *et al.*, 2004; Seneviratne *et al.*, 2006].

[34] Figure 8d shows the link between SM and α_{cloud} . In central and northern Europe, α_{cloud} does not appear to be determined by SM, suggesting a stronger influence of the (chaotic) large-scale circulation in these regions. However, in southern Europe, these two quantities are again strongly coupled: In winter, the model and observations are characterized by high SM conditions and high cloud cover (high α_{cloud}); in summer, on the other hand, they display low SM conditions and low cloud cover (low α_{cloud}). It is possible that the summer decrease in cloud cover is due to a positive feedback between SM and precipitation (lower SM leading to lower precipitation [see, e.g., Eltahir, 1998; Schär *et al.*, 1999; Betts, 2004]). However, one cannot exclude the other direction of causality, i.e., lower cloud cover caused by the large-scale circulation leading to higher E and low SM content.

4.3. Effects of Soil Moisture Limitation

[35] Now we would like to explore whether SM has a limiting effect on LE during summer in southern Europe.

RN and SM are the two quantities that mainly determine LE on climatic time scales. In contrast to the dependency of LE on SM discussed beforehand, the dependency on RN is almost linear with a small hysteresis effect (not shown). In southern Europe LE is strongly decreasing from June to August associated with decreasing SM, whereas RN is almost constant for this period (see Figure 8, bottom). This is an indication for a limiting effect of SM on LE in dry climate regions, which is indeed consistent with the results diagnosed with $\rho(\text{LE}, T_{2M})$ in Figure 7. In order to visualize this effect more clearly, Figure 9 displays LE scaled by clear-sky shortwave downward radiation (SW_{dn}^{clear}) as a function of SMI, which removes the dependence on the solar zenith angle. LE is positively correlated with SM in summer in southern Europe, whereas the corresponding scaled SW_{dn} and H fluxes are negatively correlated with SM (see Figure 9, left and middle) as a consequence of α_{cloud} increasing with SM (see Figure 8). This is suggestive of a cloud-radiation-surface coupling, with drier soils in southern Europe leading to less LE and less cloudy PBLs and, hence, more SW_{dn} and H at the surface, though, as mentioned earlier, the direction of causality cannot

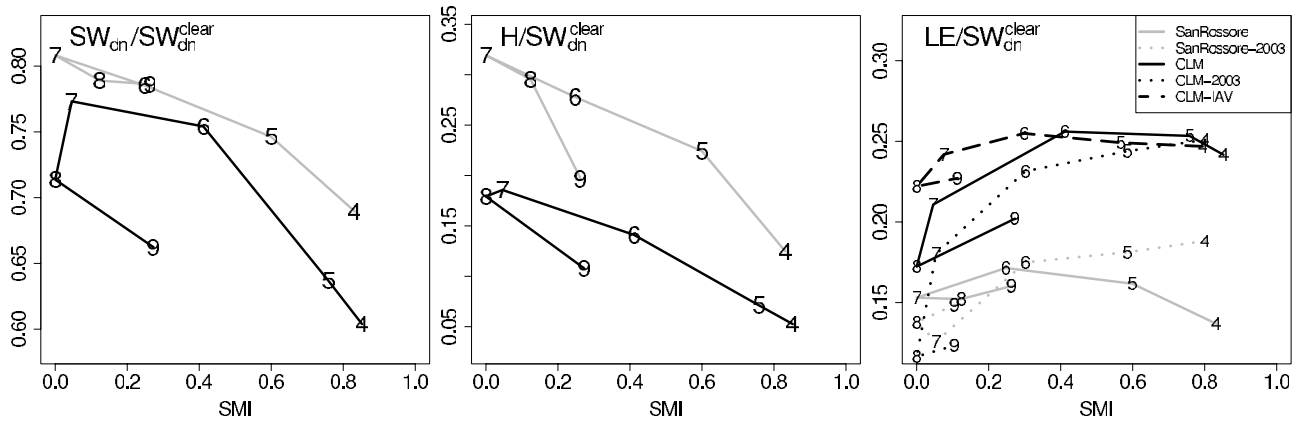


Figure 9. Mean seasonal cycle (without cold season period) of (left) SW_{dn} , (middle) H , and (right) LE scaled by SW_{dn}^{clear} (all in $W\ m^{-2}$) as a function of SMI (no unit). Shown is only San Rossore for the years 2002–2005. The LE/SW_{dn}^{clear} plot additionally gives LE scaled by SW_{dn}^{clear} for the year 2003 (exceptional summer heat wave) and LE scaled by SW_{dn}^{clear} but without soil moisture limitation (CLM simulation with removed interannual variability of SM (IAV)).

unambiguously be established. Note that this limiting effect of SM on LE is particularly strong for the exceptional 2003 heat wave and drought [e.g., Schär et al., 2004; Andersen et al., 2005; Granier et al., 2007] (see Figure 9, right). The strong T_{2M} anomaly during the 2003 summer and its representation in CLM, ECMWFop and in the E-OBS observations is depicted in Figure 10. Figure 10 shows that both CLM and ECMWFop correctly capture the heat wave, which requires some correct representation of SM limitation [e.g., Fischer et al., 2007a, 2007b]. Moreover, a corresponding CLM simulation with prescribed high SM conditions (removed interannual SM variability (CLM-IAV), i.e., prescribed climatological SM) does not show a limiting effect of SM on LE in dry periods, since SM is always above the plant wilting point (see Figure 9, right). These overall results suggest that the land-PBL-atmosphere coupling is reasonably represented in CLM and also in ECMWFop.

4.4. Seasonal Cycle of Net Radiation and Cloud Albedo Biases

[36] Before discussing the coupling of the surface energy budget components with PBL quantities on the daily time scale, an explanation is provided for the large biases in RN. Figure 11 displays the RN bias of the mean seasonal cycle together with the bias of the α_{cloud} . These biases are more or less in line with each other, with an overestimation of α_{cloud} (meaning an overestimation of the total cloud cover) and an underestimation of RN from spring to autumn, which holds for all sites (not shown). In winter, RN is still underestimated, whereas α_{cloud} is also slightly underestimated. This is an indication that RN biases are not only determined by biases in α_{cloud} , and/or that the estimation of α_{cloud} is associated with some uncertainties. However, note that clear-sky radiation as well as surface albedo (at least in summer) are reasonably modeled in CLM [see Jaeger et al., 2008, and references therein] and, hence, are not major contributors to the RN bias. The corresponding analyses for

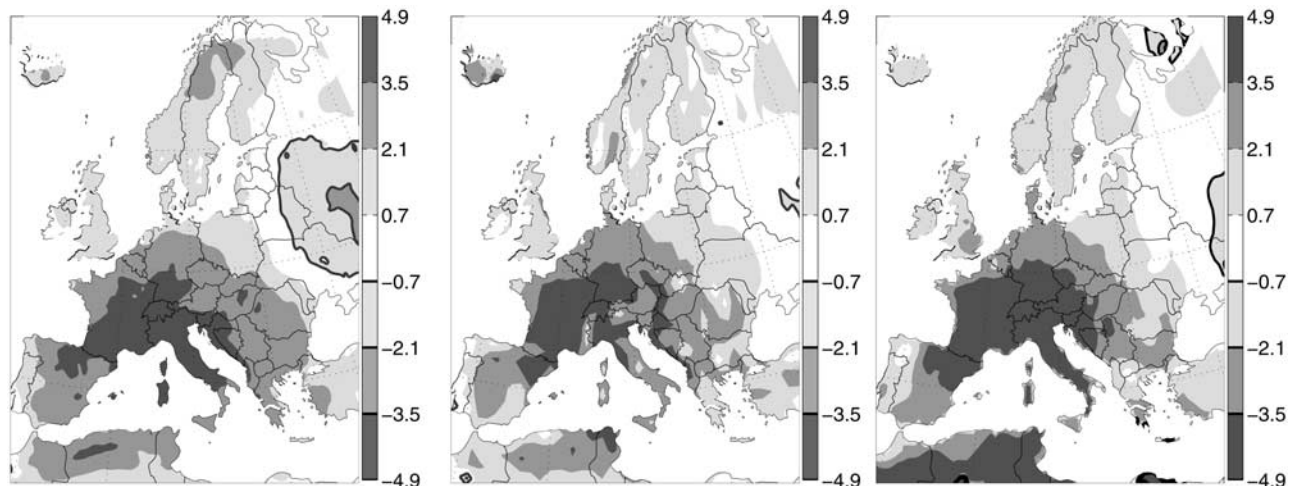


Figure 10. The 2003 summer mean T_{2M} anomaly of (left) CLM, (middle) ECMWFop, and (right) E-OBS with respect to 1960–1990. Black solid contours indicate negative anomalies.

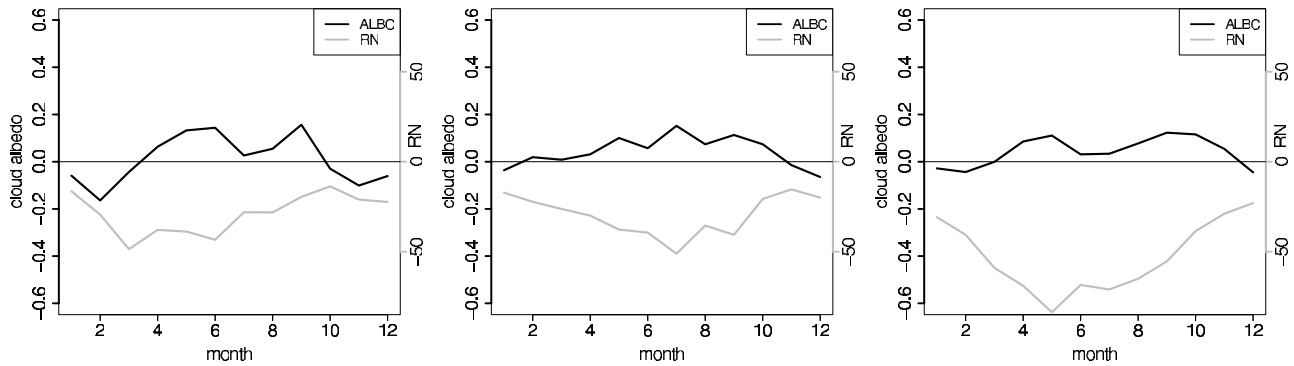


Figure 11. Mean seasonal cycle of the α_{cloud} (no unit) bias (left y axis, black line) and RN (W m^{-2}) bias (right y axis, grey line). Shown are (left) Hyytiälä, (middle) Vielsalm, and (right) San Rossore for the period 2002–2005.

ECMWFop give similar results, though RN and α_{cloud} biases are usually smaller (not shown).

4.5. Model Biases as a Function of Observed Cloud Albedo

[37] In this section, we investigate whether the models represent on the daily time scale the coupling of land-PBL-atmosphere processes that can be diagnosed from the observations. The analysis again primarily focuses on the summer season for 2002–2005 and on CLM, whereas the respective performance of ECMWFop is only briefly discussed.

[38] The daily biases of RH, T_{2M} , and α_{cloud} and RN, LE, and H are displayed in Figure 12 (top) and Figure 12

(bottom), respectively, as a function of observed daily α_{cloud} . The lines denote a fit determined by the nonparametric local polynomial regression algorithm “Loess” [Cleveland *et al.*, 1990]. In Hyytiälä, when little cloud cover is observed (α_{cloud} small), CLM exhibits an overestimation of cloud cover and a corresponding high bias in RH and low bias in T_{2M} . When the observed cloud cover is larger, the biases of CLM are reversed and generally smaller. The CLM bias of α_{cloud} is projected onto a bias of RN and H. The LE bias on the contrary appears mostly unrelated to the α_{cloud} bias. In summary, when observed cloud cover is low, CLM has too much cloud inducing low RN and H, which results in a cold, moist bias. For high observed cloud cover, the pattern is reversed but the biases are generally smaller

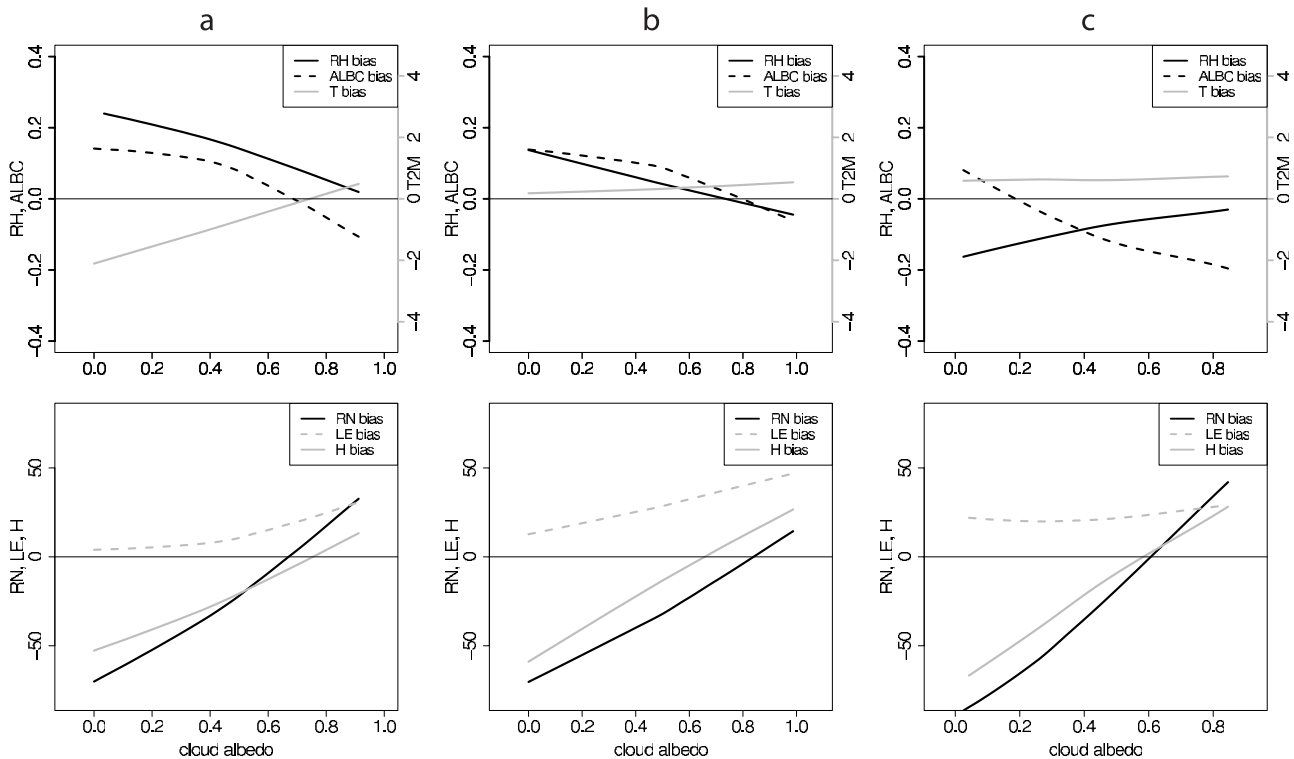


Figure 12. (top) Daily summer bias of α_{cloud} (no unit) and RH (no unit) (left y axis, black line) and T_{2M} (K) (right y axis, grey line) as a function of observed α_{cloud} . (bottom) Same but for biases of RN, LE, and H (all in W m^{-2}). Shown are (a) Hyytiälä, (b) Vielsalm, and (c) San Rossore for the period 2002–2005.

than for low cloud cover: CLM has too little cloud, and as a consequence modeled RN and H are overestimated, resulting in a warm, dry bias. These biases are very similar to those described by *Betts et al.* [2006] for ERA40 at the Canadian boreal climate station Saskatchewan. The same holds for Vielsalm, except that T_{2M} has no bias for the whole range of observed α_{cloud} . Generally, these biases are consistent except for the central Italian stations, where CLM is rather too dry and warm for all observed α_{cloud} , though RN, LE, H and α_{cloud} show similar biases as at the other stations. This might be caused, for example, by the vicinity of the stations to the Mediterranean Sea (or it might be an artefact of the fitted line). Moreover, the corresponding analysis for ECMWFop looks similar except for T_{2M} . Under low observed cloud cover, the absolute values of the respective ECMWFop biases are larger for LE (as shown before in Figure 5) but smaller for α_{cloud} , RN and RH compared to those of the CLM.

5. Summary and Conclusions

[39] In this study the surface fluxes of heat and moisture as well as the coupling of land-PBL-atmosphere processes are assessed in the CLM RCM. We use tower observations from FLUXNET and a methodology introduced by Alan K. Betts [e.g., *Betts*, 2004] for the validation. The analysis focuses on three climate zones over the European continent and on the period 2002–2005. We also compare the CLM performance with that of the ECMWFop data set and the ICTS models for part of the analysis. The main results of this study are as follows.

[40] 1. CLM displays a systematic underestimation of RN on the monthly as well as on the hourly time scale associated with an overestimation of the cloud cover. However, the missing energy is not equally distributed onto LE and H, leading to an underestimation of H, while the LE fluxes are mostly within the uncertainty range of the eddy-covariance flux measurements. The underestimation of H and correct LE leads to an underestimation of B. The systematic bias in B is in line with the known deficiency of CLM having a too shallow, too cold and often also too moist PBL in summer, if Tiedke convection scheme with moisture convergence closure is used. Larger values of the minimal stomatal resistance could partly correct for this deficiency.

[41] 2. There is a tendency for H to have a positive and LE to have a negative phase-shift error in the mean seasonal cycle. This could be an indication of a too early onset of the vegetation period in spring, though the phase shifts are small in LE, but for some stations quite large in H. In contrast, the diurnal cycle phase-shift errors are generally larger, with phase-shift errors of LE being systematically positive (up to 2 h). The same holds for RN for most stations and months, whereas phase-shift errors of H are mostly negative. Note that phase shifts in the diurnal cycle of LE and H could be critical for several aspects of land-PBL-atmosphere interactions, in particular for convective precipitation.

[42] 3. ECMWFop displays a better seasonal cycle of RN compared to CLM, though it also presents systematic underestimations compared to the FLUXNET observations (partly due to SW_{dn} underestimation). Consequently, H and

particularly LE are both larger in ECMWFop than in the CLM simulations for most stations. This corresponds to a smaller H bias in ECMWFop; however, there are some indications that LE is overestimated (see also point 4 below). As in CLM, there is a tendency in ECMWFop for H to have a positive and LE to have a negative phase-shift error compared to the FLUXNET seasonal cycles.

[43] 4. A comparison of E from basin-scale atmospheric water balance estimates with CLM reveals a good agreement for European river catchments. By contrast, ECMWFop generally overestimates E in summer as found already by *Hagemann et al.* [2005] for ERA40. This is consistent with the results of the LE validation with the FLUXNET observations (points 1 and 3 above).

[44] 5. A comparison of the seasonal cycles of RN, LE, and H in CLM with the ICTS RCMs reveals that the RN underestimation is a specific feature of the CLM model, at least partly associated with a total model cloud cover overestimation. B on the other hand appears to be underestimated in all models, though the measurement uncertainty is large.

[45] 6. In southern Europe, the FLUXNET measurements show that RN, LE and H are coupled on the monthly time scales to SM, RH and α_{cloud} , a feature that is captured both by CLM and ECMWFop. In this region, the coupling between SM, α_{cloud} and RH suggests that wet soils are associated with cloudier, moister and shallower PBLs, though the direction of causality is unclear. On the other hand, in central and northern Europe α_{cloud} seems to be determined primarily by the large-scale circulation, and is mostly unrelated to the SM field. The analysis of the correlation between evapotranspiration and temperature ($\rho(LE, T_{2M})$) similarly suggests a strong coupling between SM and LE, H and temperature in southern Europe, both in the observations and the model simulations. This is consistent with the results of previous modeling and observational studies [*Seneviratne et al.*, 2006; *Teuling et al.*, 2009].

[46] 7. On the daily time scales (particularly in summer) when the observed cloud cover is low, CLM overestimates the cloud cover, inducing an underestimation of RN and H, which results in a cold, moist bias. For high observed cloud cover, the pattern is reversed: CLM has too little clouds, and as a consequence modeled RN and H are overestimated, resulting in a warm, dry bias. Except for the T_{2M} bias, the corresponding analysis for ECMWFop looks similar (consistent with biases found by *Betts et al.* [2006] for ERA40). This indicates a lack of sensitivity of the cloud cover in both models, possibly due to underestimated positive feedbacks.

[47] In conclusion, this analysis has shown that the land-PBL-atmosphere coupling is reasonably represented both in CLM and ECMWFop, despite some identified biases, mostly in the cloud cover. A significant deficiency of CLM is its RN underestimation with serious consequences for H, B and the whole PBL structure. However, several other current state-of-the-art RCMs (ICTS simulations) show similar deficiencies for B and the surface fluxes of heat and moisture. Despite large and systematic errors in RN, precipitation and T_{2M} are reasonably represented in CLM versions 2.4.11 and 2.4.6 [*Jaeger et al.*, 2008]. The present analysis shows that CLM also simulates LE reasonably, and correctly captures regions of strong SM limitations on LE. In addition, this analysis has shown how FLUXNET

observations can be utilized to help diagnose land surface and PBL biases in climate models. Further studies addressing these aspects for a larger number of models would help to characterize the uncertainty in the representation of these processes, and to identify perspectives for their improvement for the computation of reliable climate scenarios.

[48] **Acknowledgments.** This research was supported through the EU-project CECILIA and ETH Zurich. The simulations of ETH have been conducted at the Swiss National Supercomputing Centre (CSCS). We are indebted to the COSMO and CLM community, as well as to MeteoSwiss and ECMWF, for providing access to and support for the CLM and ECMWFop, respectively. For the access to the FLUXNET data, we would like to thank the following PIs and their collaborators: Michael Marek (CZBK1), Riccardo Valentini (ITCpz, ITAmp), André Granier (FRHes), Timo Vesala (FIHyy), Tuomas Laurila (FIKaa, FISod), Serge Rambal (FRPue), Stefano Minerbi (ITRen), Guenther Seufert (ITSRo), Marc Aubinet (BEVie), and Martin Heimann (RUFyo). We are particularly indebted to Leonardo Montagnani and Stefano Minerbi (ITRen) for useful comments on the paper. Discussions with Thierry Corti, Irene Lehner, Felix Ament, Cathy Hohenegger, Peter Brockhaus, Andreas Roesch, and Martin Hirschi were highly appreciated. Moreover, we are grateful to Daniel Lüthi for technical support. We acknowledge the E-OBS data set from the EU-FP6 project ENSEMBLES (<http://www.ensembles-eu.org>) and the data providers in the ECA&D project (<http://eca.knmi.nl>).

References

- Andersen, O. B., S. I. Seneviratne, J. Hinderer, and P. Viterbo (2005), GRACE-derived terrestrial water storage depletion associated with the 2003 European heat wave, *Geophys. Res. Lett.*, *32*, L18405, doi:10.1029/2005GL023574.
- Aubinet, M., B. Chermanne, M. Vandenhaute, B. Longdoz, M. Yernaux, and E. Laitat (2001), Long term carbon dioxide exchange above a mixed forest in the Belgian Ardennes, *Agric. For. Meteorol.*, *108*, 293–315.
- Baldocchi, D. (2008), Breathing of the terrestrial biosphere: lessons learned from a global network of carbon dioxide flux measurement systems, *Aust. J. Bot.*, *56*, 1–26.
- Baldocchi, D., et al. (2001), FLUXNET: A new tool to study the temporal and spatial variability of ecosystem-scale carbon dioxide, water vapor, and energy flux densities, *Bull. Am. Meteorol. Soc.*, *82*, 2415–2433.
- Betts, A. K. (2004), Understanding hydrometeorology using global models, *Bull. Am. Meteorol. Soc.*, *85*, 1673–1688.
- Betts, A. K. (2007), Coupling of water vapor convergence, clouds, precipitation, and land-surface processes, *J. Geophys. Res.*, *112*, D10108, doi:10.1029/2006JD008191.
- Betts, A. K., and P. Viterbo (2005), Land-surface, boundary layer and cloud-field coupling over the southwestern Amazon in ERA-40, *J. Geophys. Res.*, *110*, D14108, doi:10.1029/2004JD005702.
- Betts, A. K., J. Ball, A. Barr, T. A. Black, J. H. McCaughey, and P. Viterbo (2006), Assessing land-surface-atmosphere coupling in the ERA-40 reanalysis with boreal forest data, *Agric. For. Meteorol.*, *140*, 355–382, doi:10.1016/j.agrformet.2006.08.009.
- Brockhaus, P., D. Lüthi, and C. Schär (2008), Aspects of the diurnal cycle in a regional climate model, *Meteorol. Z.*, *17*, 433–443.
- Christensen, J. H., and O. B. Christensen (2003), Severe summertime flooding in Europe, *Nature*, *421*, 805–806.
- Cleveland, R. B., W. S. Cleveland, J. E. McRae, and I. Terpenning (1990), STL: A seasonal-trend decomposition procedure based on Loess, *J. Off. Stat.*, *6*, 3–33.
- Dickinson, R. E. (1984), Modeling evapotranspiration for the three-dimensional global climate models, in *Climate Processes and Climate Sensitivity*, *Geophys. Monogr. Ser.*, vol. 29, edited by J. E. Hansons and T. Takahashi, pp. 58–72, AGU, Washington, D. C.
- Ek, M. B., and A. A. M. Holtslag (2004), Influence of soil moisture on boundary layer cloud development, *J. Hydrometeorol.*, *5*, 86–99.
- Eltahir, E. A. B. (1998), A soil moisture-rainfall feedback mechanism: 1. Theory and observations, *Water Resour. Res.*, *34*, 765–776.
- Findell, K. L., and E. A. B. Eltahir (2003a), Atmospheric controls on soil moisture-boundary layer interactions. Part I: Framework development, *J. Hydrometeorol.*, *4*, 552–569.
- Findell, K. L., and E. A. B. Eltahir (2003b), Atmospheric controls on soil moisture-boundary layer interactions. Part II: Feedbacks within the continental United States, *J. Hydrometeorol.*, *4*, 570–583.
- Finkelstein, P. L., and P. F. Sims (2001), Sampling error in eddy correlation flux measurements, *J. Geophys. Res.*, *106*, 3503–3509.
- Fischer, E. M., and C. Schär (2009), Future changes in daily summer temperature variability: driving processes and role for temperature extremes, *Clim. Dyn.*, doi:10.1007/s00382-008-0473-8, in press.
- Fischer, E. M., S. I. Seneviratne, D. Lüthi, and C. Schär (2007a), Contribution of land-atmosphere coupling to recent European summer heat waves, *Geophys. Res. Lett.*, *34*, L06707, doi:10.1029/2006GL029068.
- Fischer, E. M., S. I. Seneviratne, P. L. Vidale, D. Lüthi, and C. Schär (2007b), Soil moisture–atmosphere interactions during the 2003 European summer heat wave, *J. Clim.*, *20*, 5081–5099.
- Foken, T. (2008), The energy balance closure problem—An overview, *Ecol. Appl.*, *18*, 114–130.
- Frei, C., R. Schöll, S. Fukutome, J. Schmidli, and P. L. Vidale (2006), Future change of precipitation extremes in Europe: Intercomparison of scenarios from regional climate models, *J. Geophys. Res.*, *111*, D06105, doi:10.1029/2005JD005965.
- Gilgen, H., and A. Ohmura (1999), The Global Energy Balance Archive (GEBA), *Bull. Am. Meteorol. Soc.*, *80*, 831–850.
- Gilmanov, T. G., et al. (2007), Partitioning European grassland net ecosystem CO₂ exchange into gross primary productivity and ecosystem respiration using light response function analysis, *Agric. Ecosyst. Environ.*, *121*, 93–120.
- Granier, A., et al. (2000), The carbon balance of a young beech forest, *Funct. Ecol.*, *14*, 312–325.
- Granier, A., et al. (2007), Evidence for soil water control on carbon and water dynamics in European forests during the extremely dry year: 2003, *Agric. For. Meteorol.*, *143*, 123–145.
- Hagemann, S., K. Arpe, and L. Bengtsson (2005), Validation of the hydrological cycle of ERA40, *ECMWF ERA-40 Proj. Rep. 24*, 42 pp., Eur. Cent. for Medium-Range Weather Forecasts, Reading, U. K. (Available at <http://www.ecmwf.int/publications>)
- Hatakka, J., et al. (2003), Overview of the atmospheric research activities and results at Pallas GAW station, *Boreal Environ. Res.*, *8*, 365–383.
- Haylock, M. R., N. Hofstra, A. M. G. Klein Tank, E. J. Klok, P. D. Jones, and M. New (2008), A European daily high-resolution gridded dataset of surface temperature and precipitation, *J. Geophys. Res.*, *113*, D20119, doi:10.1029/2008JD010201.
- Hirschi, M., S. I. Seneviratne, and C. Schär (2006a), Seasonal variations in terrestrial water storage for major mid-latitude river basins, *J. Hydrometeorol.*, *7*, 39–60.
- Hirschi, M., P. Viterbo, and S. I. Seneviratne (2006b), Basin-scale water-balance estimates of terrestrial water storage variations from ECMWF operational forecast analysis, *Geophys. Res. Lett.*, *33*, L21401, doi:10.1029/2006GL027659.
- Hirschi, M., S. I. Seneviratne, S. Hagemann, and C. Schär (2007), Analysis of seasonal terrestrial water storage variations in regional climate simulations over Europe, *J. Geophys. Res.*, *112*, D22109, doi:10.1029/2006JD008338.
- Hohenegger, C., P. Brockhaus, C. Bretherton, and C. Schär (2009), The soil moisture precipitation feedback in simulations with explicit and parameterized convection, *J. Clim.*, in press.
- Intergovernmental Panel on Climate Change (IPCC) (2007), *Climate Change 2007: The Physical Science Basis. Contribution of Working Group I to the Fourth Assessment Report of the Intergovernmental Panel on Climate Change*, edited by S. Solomon et al., 996 pp., Cambridge Univ. Press, Cambridge, U. K.
- Jaeger, E. B., I. Anders, D. Lüthi, B. Rockel, C. Schär, and S. I. Seneviratne (2008), Analysis of ERA40-driven CLM simulations for Europe, *Meteorol. Z.*, *17*, 349–367.
- Kjellström, E., L. Bärring, D. Jacob, R. Jones, G. Lenderink, and C. Schär (2007), Modelling daily temperature extremes: Recent climate and future changes over Europe, *Clim. Change*, *81*, 249–265.
- Koster, R. D., et al. (2004), Regions of strong coupling between soil moisture and precipitation, *Science*, *305*, 1138–1140.
- Koster, R. D., et al. (2006), GLACE: The Global Land-Atmosphere Coupling Experiment. Part I: Overview, *J. Hydrometeorol.*, *7*, 590–610.
- Koster, R. D., S. D. Schubert, and M. J. Suarez (2009), Analyzing the concurrence of meteorological droughts and warm periods, with implications for the determination of evaporative regime, *J. Clim.*, *22*, 3331–3341.
- Laurila, T., H. Soegaard, C. R. Lloyd, M. Aurela, J. P. Tuovinen, and C. Nordstroem (2001), Seasonal variations of net CO₂ exchange in European Arctic ecosystems, *Theor. Appl. Climatol.*, *70*, 183–201.
- Lenderink, G., A. van Ulden, B. van den Hurk, and E. van Meijgaard (2007), Summertime inter-annual temperature variability in an ensemble of regional model simulations: Analysis of the surface energy budget, *Clim. Change*, *81*, 233–247.
- Marcolla, B., A. Cescatti, L. Montagnani, G. Manca, G. Kerschbaumer, and S. Minerbi (2005), Importance of advection in the atmospheric CO₂ exchanges of an alpine forest, *Agric. For. Meteorol.*, *130*, 193–206.

- Meehl, G. A., and C. Tebaldi (2004), More intense, more frequent, and longer lasting heat waves in the 21st century, *Science*, *305*, 994–997.
- Milyukova, I. M., O. Kolle, A. V. Varlagin, N. N. Vygodskaya, E. D. F. Schulze, and J. Lloyd (2002), Carbon balance of a southern taiga spruce stand in European Russia, *Tellus, Ser. B*, *54*, 429–442.
- Pal, J. S., F. Giorgi, and X. Bi (2004), Consistency of recent European summer precipitation trends and extremes with future regional climate projections, *Geophys. Res. Lett.*, *31*, L13202, doi:10.1029/2004GL019836.
- Raschendorfer, M. (2001), The new turbulence parametrization of LM, *COSMO Newsl.*, *1*, 90–98.
- Reda, I., and A. Andreas (2003), Solar position algorithm for solar radiation application, *Tech. Rep. NREL/TP-560-34302*, 56 pp., Natl. Renewable Energy Lab., Golden, Colo.
- Reichstein, M., et al. (2002), Severe drought effects on ecosystem CO₂ and H₂O fluxes at three Mediterranean evergreen sites: Revision of current hypotheses?, *Global Change Biol.*, *8*, 999–1017.
- Reichstein, M., et al. (2005), On the separation of net ecosystem exchange into assimilation and ecosystem respiration: Review and improved algorithm, *Global Change Biol.*, *11*, 1424–1439.
- Richardson, A. D., et al. (2006), A multi-site analysis of random error in tower-based measurements of carbon and energy fluxes, *Agric. For. Meteorol.*, *136*, 1–18.
- Ritter, B., and J. F. Geleyn (1992), A comprehensive radiation scheme of numerical weather prediction with potential application to climate simulations, *Mon. Weather Rev.*, *120*, 303–325.
- Rockel, B., I. Meinke, L. Roads, W. J. Gutowski, R. W. Arritt, E. S. Takle, and C. Jones (2006), The Inter-CSE Transferability Study, *CEOP Newsl.*, *8*, 4–5.
- Schär, C., D. Lüthi, U. Beyerle, and E. Heise (1999), The soil-precipitation feedback: A process study with a regional climate model, *J. Clim.*, *12*, 722–741.
- Schär, C., P. L. Vidale, D. Lüthi, C. Frei, C. Häberli, M. A. Liniger, and C. Appenzeller (2004), The role of increasing temperature variability in European summer heatwaves, *Nature*, *427*, 332–336.
- Schmid, H. P., H.-B. Su, C. S. Vogel, and P. S. Curtis (2003), Ecosystem atmosphere exchange of carbon dioxide over a mixed hardwood forest in northern lower Michigan, *J. Geophys. Res.*, *108*(D14), 4417, doi:10.1029/2002JD003011.
- Schrodin, R., and E. Heise (2002), A new multi-layer soil model, *COSMO Newsl.*, *2*, 149–151.
- Seneviratne, S. I., and R. Stöckli (2008), The role of land-atmosphere interactions for climate variability in Europe, in *Climate Variability and Extremes During the Past 100 Years*, *Adv. Global Change Res.*, vol. 33, edited by S. Brönnimann et al., Springer, New York.
- Seneviratne, S. I., P. Viterbo, D. Lüthi, and C. Schär (2004), Inferring changes in terrestrial water storage using ERA-40 reanalysis data: The Mississippi River basin, *J. Clim.*, *17*, 2039–2057.
- Seneviratne, S. I., D. Lüthi, M. Litschi, and C. Schär (2006), Land-atmosphere coupling and climate change in Europe, *Nature*, *443*, 205–209.
- Stappeler, J., G. Dom, U. Schättler, H. W. Bitzer, A. Gassmann, U. Damrath, and G. Gregoric (2003), Meso-gamma scale forecasts using the nonhydrostatic model LM, *Meteorol. Atmos. Phys.*, *82*, 75–96.
- Stöckli, R., D. M. Lawrence, G.-Y. Niu, K. W. Oleson, P. E. Thornton, Z.-L. Yang, G. B. Bonan, A. S. Denning, and S. W. Running (2008), Use of FLUXNET in the Community Land Model development, *J. Geophys. Res.*, *113*, G01025, doi:10.1029/2007JG000562.
- Suni, T., J. Rinne, A. Reissel, N. Altimir, P. Keronen, Ü. Rannik, M. D. Maso, M. Kulmala, and T. Vesala (2003), Long-term measurements of surface fluxes above a Scots pine forest in Hyytiälä, southern Finland, 1996–2001, *Boreal Environ. Res.*, *4*, 287–301.
- Takle, E. S., J. Roads, B. Rockel, W. J. Gutowski, R. W. Arritt, I. Meinke, C. G. Jones, and A. Zadra (2007), Transferability intercomparison: An opportunity for new insight on the global water cycle and energy budget, *Bull. Am. Meteorol. Soc.*, *88*, 375–384.
- Teuling, A. J., et al. (2009), A regional perspective on trends in continental evaporation, *Geophys. Res. Lett.*, *36*, L02404, doi:10.1029/2008GL036584.
- Tiedtke, M. (1989), A comprehensive mass flux scheme for cumulus parameterization in large-scale models, *Mon. Weather Rev.*, *117*, 1779–1800.
- Twine, T. E., W. P. Kustas, J. M. Norman, D. R. Cook, P. R. Houser, T. P. Meyers, J. H. Prueger, P. J. Starks, and M. L. Wesely (2000), Correcting eddy-covariance flux underestimates over a grassland, *Agric. For. Meteorol.*, *103*, 279–300.
- Uppala, S. M., et al. (2005), The ERA-40 reanalysis, *Q. J. R. Meteorol. Soc.*, *131*, 2961–3012.
- Vidale, P. L., D. Lüthi, R. Wegmann, and C. Schär (2007), European summer climate variability in a heterogeneous multi-model ensemble, *Clim. Change*, *81*, 209–232.
- Wilson, K., et al. (2002), Energy balance closure at FLUXNET sites, *Agric. For. Meteorol.*, *113*, 223–243.
- Yeh, P. J. F., M. Irizzary, and E. A. B. Eltahir (1998), Hydroclimatology of Illinois: A comparison of the estimates of evaporation based on atmospheric water balance and soil water balance, *J. Geophys. Res.*, *103*, 19,823–19,837.
- Young, A. T. (1994), Air mass and refraction, *Appl. Opt.*, *33*, 1108–1110.

E. B. Jaeger and S. I. Seneviratne, Institute for Atmospheric and Climate Science, ETH Zurich, Universitätstrasse 16, CH-8092 Zurich, Switzerland. (eric.jaeger@env.ethz.ch)

R. Stöckli, Climate Analysis, Climate Services, MeteoSwiss, Krähbühlstrasse 58, CH-8044 Zurich, Switzerland.